Pergamon

Geochimica et Cosmochimica Acta, Vol. 66, No. 10, pp. 1839–1850, 2002

0016-7037/02 $22.00 + .00

PII S0016-7037(01)00881-X

Energetics of anhydrite, barite, celestine, and anglesite: A high-temperature and differential scanning calorimetry study

J. MAJZLAN,* A. NAVROTSKY, and J. M. NEIL

Thermochemistry Facility, Department of Geology, University of California at Davis, Davis, CA 95616, USA

(*Received June* 18, 2001; *accepted in revised form November* 28, 2001)

Abstract—The thermochemistry of anhydrous sulfates (anglesite, anhydrite, arcanite, barite, celestine) was investigated by high-temperature oxide melt calorimetry and differential scanning calorimetry. Complete retention and uniform speciation of sulfur in the solvent was documented by (a) chemical analyses of the solvent ($3Na_2O \cdot 4MoO_3$) with dissolved sulfates, (b) Fourier transform infrared spectroscopy confirming the absence of sulfur species in the gases above the solvent, and (c) consistency of experimental determination of the enthalpy of drop solution of SO_3 in the solvent. Thus, the principal conclusion of this study is that high-temperature oxide melt calorimetry with $3Na_2O \cdot 4MoO_3$ solvent is a valid technique for measurement of enthalpies of formation of anhydrous sulfates. Enthalpies of formation (in kJ/mol) from the elements (ΔH_f^o) were determined for synthetic anhydrite ($CaSO_4$) (-1433.8 ± 3.2), celestine ($SrSO_4$) (-1452.1 ± 3.3), anglesite ($PbSO_4$) (-909.9 ± 3.4), and two natural barite ($BaSO_4$) samples (-1464.2 ± 3.7, -1464.9 ± 3.7). The heat capacity of anhydrite, barite, and celestine was measured between 245 and 1100 K, with low- and high-temperature Netzsch (DSC-404) differential scanning calorimeters. The results for each sample were fitted to a Haas-Fisher polynomial of the form $C_p(245\ K < T < 1100\ K) = a + bT + cT^{-2} + dT^{-0.5} + eT^2$. The coefficients of the equation are as follows: for anhydrite $a = 409.7$, $b = -1.764 \times 10^{-1}$, $c = 2.672 \times 10^6$, $d = -5.130 \times 10^3$, $e = 8.460 \times 10^{-5}$; for barite, $a = 230.5$, $b = -0.7395 \times 10^{-1}$, $c = -1.170 \times 10^6$, $d = -1.587 \times 10^3$, $e = 4.784 \times 10^{-5}$; and for celestine, $a = 82.1$, $b = 0.8831 \times 10^{-1}$, $c = -1.213 \times 10^6$, $d = 0.1890 \times 10^3$, $e = -1.449 \times 10^{-5}$. The 95% confidence interval of the measured C_p varies from 1 to 2% of the measured value at low temperature up to 2 to 5% at high temperature. The measured thermochemical data improve or augment the thermodynamic database for anhydrous sulfates and highlight the remaining discrepancies. *Copyright © 2002 Elsevier Science Ltd*

1. INTRODUCTION

The motivation for this study is to test high-temperature oxide melt calorimetry as a new tool for studying the energetics of sulfates. Sulfates of Ba, Sr, Pb, Ca and their solid solutions, and the jarosite–alunite group minerals are of interest to geologists and geochemists (e.g., Rimstidt, 1997; Myneni, 2000), and material scientists (e.g., Brobst, 1983; Dutrizac and Jambor, 2000). A significant amount of thermodynamic data on the jarosite–alunite group minerals (Härtig et al., 1984; Stoffregen, 1993; Baron and Palmer, 1996) and barite–celestine–anglesite end members and their solid solutions (Brower and Renault, 1977; Nordstrom and Munoz, 1994; Becker et al., 2000; Kotel'nikov et al., 2000) has been amassed; however, discrepancies and inconsistencies remain in abundance. High-temperature oxide melt calorimetry has previously been successfully applied to a variety of synthetic phases and minerals (Navrotsky, 1997), and the technique should be capable of eliminating some of the problems in the thermodynamics of sulfates. Moreover, thermodynamic data can serve to constrain interatomic potentials in sulfates for use in theoretical calculations and modeling (Becker et al., 2000) or to predict thermodynamic properties of other sulfates in combination with crystallographic studies (Hawthorne et al., 2000)

The second objective of this study is an evaluation and comparison of the thermodynamic data acquired in this study to the existing data. For this study, we have selected the anhydrous sulfates anglesite ($PbSO_4$), anhydrite ($CaSO_4$), arcanite (K_2SO_4), barite ($BaSO_4$), and celestine ($SrSO_4$) because of their simple chemical composition, ease of handling, and presumed availability of reliable thermodynamic data. A detailed literature review revealed discrepancies and gaps in the thermodynamic data even for well-studied sulfates, including the ones selected for this study.

2. MATERIALS AND METHODS

2.1. Synthetic Samples

Samples for thermodynamic measurements must be phase pure, well crystalline, and devoid of inclusions. Rapid precipitation of sparingly soluble sulfates from aqueous solutions tends to trap impurities (solution, hydroxides, carbonates). Other samples can be water sensitive or show extensive polymorphism. Therefore, great care was taken to synthesize satisfactory material for calorimetry. The chemicals, their purity, and the sources used for the calorimetric investigation are listed in Table 1. Lead nitrate, used for the synthesis of anglesite, was prepared by dissolution of PbO in excess nitric acid and several cycles of crystallization and dissolution in deionized water. Potassium sulfate (arcanite) was purified by dissolution in deionized water and crystallization of large single crystals (up to 5 mm). Barium and strontium carbonates were loaded into a gold crucible and purified in a stream of CO_2 at 1273 K for 3 d. Water-free K_2CO_3 was prepared by heating hydrated potassium carbonate in a gold crucible in vacuum at 873 K overnight. The sample was transferred to a glove box under vacuum and retrieved from the gold crucible in an argon atmosphere. The gold crucible used for the purification was cleaned before each run by boiling in 0.1 mol/L HCl and rinsing in deionized water. Calcium oxide was heated in air at 1373 K for 4 h in a platinum crucible, and

* Author to whom correspondence should be addressed (jmajzlan@ucdavis.edu).

Table 1. Chemicals, their purity, and their source, used in calorimetry or for synthesis of samples for calorimetry.

Chemical	Purity	Supplier
$Sr(NO_3)_2$	≥99.0%	Alfa Aesar
$Ba(NO_3)_2$	99.999% metals basis	Alfa Aesar
$Ca(NO_3)_2.4H_2O$	99.5%	Fisher
PbO (massicot)	99.9995%	Johnson Matthey
CaO (lime)	99.95% metals basis	Alfa Aesar
$BaCO_3$ (witherite)	99.95% metals basis	Alfa Aesar
$SrCO_3$ (strontianite)	99.994% metals basis	Alfa Aesar
$PbCO_3$ (cerussite)	99.999% metals basis	Alfa Aesar
K_2CO_3	99.7% (assay)	Fisher
$Na_2MoO_4 \cdot 2H_2O$	100.2% (assay)	Fisher
Na_2SO_4	99.2% (assay)	Fisher
K_2SO_4 (arcanite)	99.3% (assay)	Fisher
α-Fe_2O_3 (hematite)	99.999%	Johnson Matthey
α-SiO_2 (quartz)	>99.5%	Fluka

transferred into and thereafter stored in a glove box in an argon atmosphere (<1 ppm H_2O).

Tetragonal PbO was synthesized in a hydrothermal furnace. Approximately 100 mg of starting material (mostly orthorhombic PbO) were loaded into a gold capsule (internal volume ~1.6 mL), together with 0.9 mL of 1 mol/L NaOH. The solution was prepared from triply deionized water through which N_2 was bubbled for 1 h to remove dissolved CO_2. The capsule was welded shut and inserted into the hydrothermal furnace with water as the pressure medium; the temperature was cycled six times between 500 and 700 K for 2 d. Numerous crystals, up to 2-mm platelets, were retrieved from the capsule, washed several times in deionized water, and dried at 340 K in air. Lead molybdate was prepared by rapid precipitation from Na_2MoO_4 and $Pb(NO_3)_2$ solutions and repeated washing with deionized water.

Crystals of the sparingly soluble sulfates (gypsum, anglesite, barite, celestine) were grown by the method outlined by Fernelius and Detling (1934). Solutions (12 mL, 0.1 mol/L) of sodium sulfate and the metal nitrate were poured into separate wide-mouthed test tubes that were placed upright inside a 1000-mL Pyrex beaker. The openings were sealed with a dialysis membrane, and the beaker was filled with deionized water. Slow diffusion of ions from the test tubes resulted in growth of macroscopic (several millimeters in size) crystals of the sulfates (Fig. 1). In some cases, however, we had to pierce the membranes to induce more vigorous mixing and to commence nucleation. After 4 to 6 weeks, the crystals were separated from the solution and washed up to 10 times with deionized water. Anhydrite was prepared by heating the synthetic gypsum at 773 K in air for 3 d in a platinum crucible. The photographs of the synthetic sulfate crystals were taken with a FEI XL-30sFEG electron microscope.

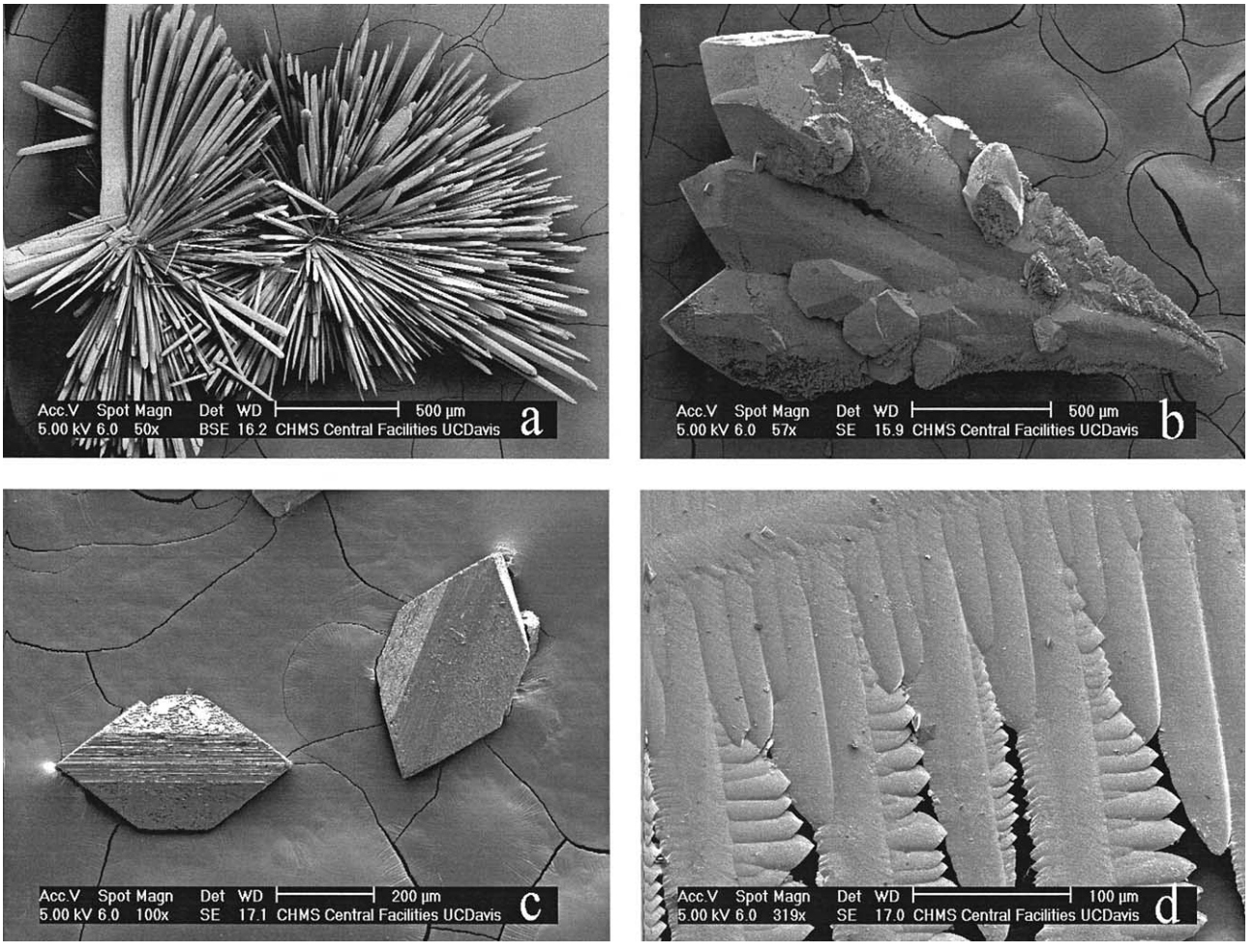

Fig. 1. Scanning electron micrographs of (a) needlelike gypsum crystals, (b) a group of celestine crystals, (c) anglesite crystals, and (d) a dendritic barite crystal. The main spine of the crystal is in the upper left corner of the photograph.

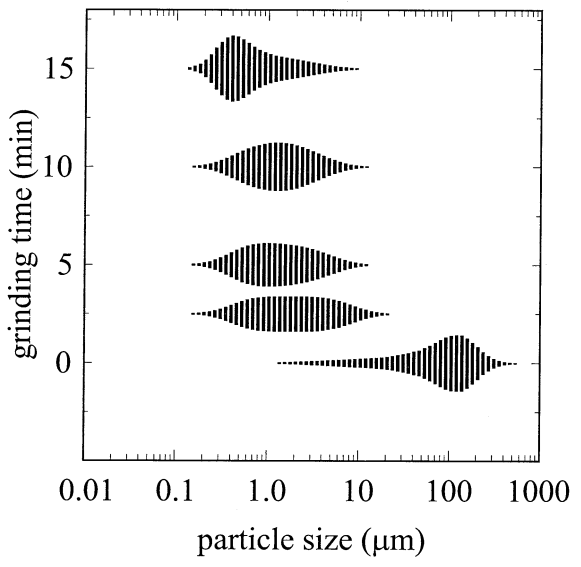

Fig. 2. Particle size of barite as a function of grinding time in McCrone micronizing mill, starting with hand-ground sample (time zero).

2.2. Natural Samples

Two natural barite samples, from the Kings Creek deposit, South Carolina (Horton, 1989), and Sterling, Colorado (Bennett, 1986), were also used in this study. The samples were crushed, and grains 0.1 to 1.0 mm in diameter were separated by dry sieving. The samples were hand-picked under a binocular microscope. The Kings Creek barite was white and coarse-grained, with a minor amount of muscovite. Muscovite was associated with fine-grained recrystallized barite along fractures and was easily separated from the rest of the sample. The Sterling barite was a large ($5 \times 2 \times 2$ cm) cleaved piece of colorless translucent barite. A small portion of the barite crystal contained iron oxide coatings; these were removed by hand-picking the crushed sample. The samples were cleaned in 1 mol/L H_2SO_4 at 313 K for 2 h, then for 20 min in boiling deionized water. They were dried by heating overnight at 773 K, then finely ground in a corundum mortar. A few grains of both samples were analyzed with a Cameca electron microprobe; we used $BaSO_4$ (Ba,S) and $SrSO_4$ (Sr) as standards, an accelerating voltage of 20 kV, a current of 10 nA, a beam size of 10 μm, and a counting time of 10 s for each analyte.

2.3. X-ray Diffraction

In preparation for X-ray diffraction (XRD) analysis and subsequent Rietveld refinement, the samples (~200 mg of powder and 7 mL of acetone) were ground for 2 min in a McCrone micronizing mill with agate grinding elements. The time necessary to grind the samples (2 min) to the desired size (1 to 10 μm) was optimized by measurement of barite (natural sample of unknown origin) particle size as a function of grinding time (Fig. 2), with a laser-scattering particle size distribution analyzer Horiba LA-910. The samples were then back-loaded into a rectangular (20×4 mm) cavity. A frosted glass slide was used as the front surface to minimize preferred orientation. The front side of the sample mount was made of a silicon monocrystal cut along (111). XRD patterns were collected with a Scintag PAD V diffractometer with Cu Kα radiation, starting at 16 to 22 °2Θ (depending on the position of the first diffraction maximum) up to 80 °2Θ with a step size of 0.02 °2Θ and dwell time of 12 s. The counting time was chosen to obtain a counting rate of several thousands of counts on the most intensive diffraction maximum. Lattice parameters of the sulfates were determined by Rietveld refinement with the GSAS software package (Larson and von Dreele, 1994). In each Rietveld refinement, the Si (111) peak (27.7 to 29.2 °2Θ) was excluded.

A special procedure was followed to collect the patterns of hygroscopic samples. K_2CO_3 was loaded into a 0.5-mm silica glass capillary inside the glove box, sealed with silicon grease, and analyzed with an Inel XRG 3000 diffractometer. The pattern corresponds to that of anhydrous K_2CO_3, thus verifying that all water was removed from the hydrated carbonate sample during the treatment. CaO was sealed in a plastic bag, and the pattern, taken with the Scintag PAD V diffractometer, corresponded to that of anhydrous CaO.

2.4. High-Temperature Calorimetry

High-temperature oxide melt calorimetry has been described in detail by Navrotsky (1997). The evaluation of experimental data requires empirical calibration using ~5 mg pellets of α-Al_2O_3 (Alfa Aesar, 99.997 wt% metals basis). The samples, in the form of ~5-mg pellets, were dropped into an empty Pt crucible at 975 or 1075 K or dissolved in the calorimetric solvent ($3Na_2O \cdot 4MoO_3$) at 975 K. In the former experiment, heat content (H_{975}-H_{298} or H_{1075}-H_{298}) was measured. In the latter, the measured heat effect is the heat of drop solution (ΔH_{dsol}), the sum of heat content (H_{975}-H_{298}) and heat of solution (ΔH_{sol}) at 975 K. An oxidizing atmosphere inside the calorimeter, intended to prevent sulfur reduction, was maintained by flushing the calorimetric assembly with oxygen (65 mL/min), and when solvent was present, also by bubbling oxygen (5 mL/min) through the solvent.

The solubility and rate of dissolution of sulfates was checked in 5 g of molten solvent in a platinum crucible at 973 K in a muffle furnace. Pellets (~5 mg) of powdered sulfates dissolved completely in approximately 10 min. A steady state of the calorimeter was reestablished 30 to 40 min after the beginning of the experiment.

2.5. Fourier Transform Infrared Spectroscopy

The gases evolved during sample dissolution in the calorimetric solvent were probed with a Bruker Equinox 55 Fourier transform infrared (FTIR) spectrometer. Because neither the high-temperature calorimeter nor the spectrometer is portable, a miniaturize calorimetric assembly was built to simulate the operation of the calorimeter. The assembly was loaded with a Pt crucible, either empty or with a solvent, and heated at 973 K. The assembly was flushed with argon (90 cm^3/min) and oxygen (10 cm^3/min), in contrast with the pure oxygen flow during the actual calorimetric experiments. Pure oxygen flow was not used to avoid damage of the ZnSe windows in the gas cell. The argon–oxygen mixture served as a carrier gas for the gases evolved during the experiment.

Table 2. Lattice parameters (Å) of the sulfate samples and statistics of the Rietveld refinement.

Sample	a	b	c	χ^2	wR_p
Anglesite	6.9581(3)	8.4788(4)	5.3976(3)	3.63	0.1287
Anhydrite	7.0024(3)	6.9931(3)	6.2416(2)	2.34	0.1265
Arcanite	7.4804(2)	10.0775(3)	5.7735(2)	2.19	0.1330
Barite (Colorado)	7.1420(4)	8.8544(6)	5.4529(4)	2.23	0.1405
Barite (South Carolina)	7.1435(5)	8.8576(7)	5.4527(4)	1.99	0.1354
Barite (synthetic)	7.1580(3)	8.8954(4)	5.4525(2)	2.02	0.1684
Celestine	6.8697(3)	8.3650(3)	5.3511(2)	2.66	0.1055

Table 3. Chemical composition of natural barite samples (in wt%), as determined by electron microprobe.

Composition	Barite (Colorado)	Barite (South Carolina)
	n = 14	n = 9
BaO	34.6[a] ± 0.3[b]	35.9 ± 0.5
SrO	2.2 ± 0.1	1.9 ± 0.2
SO_3	63.2 ± 0.4	63.4 ± 0.5
Total	99.9 ± 0.5	99.7 ± 0.8

[a] Average.
[b] Two standard deviations of the mean.

2.6. Differential Scanning Calorimetry and Thermogravimetric Analysis

Differential scanning calorimetry (DSC) experiments have been performed with Netzsch DSC-404 differential scanning calorimeters. The DSC used for low-temperature measurement has E-type thermocouples and can be operated over a temperature range of 240 to 700 K. Cooling is provided by liquid nitrogen boil-off. The high-temperature DSC has S-type thermocouples and can be operated from 300 to 1770 K. The temperature calibration was performed at the melting points of triply deionized water, indium, tin, lead, zinc, aluminum, silver, and gold. A sapphire disk supplied by the manufacturer was used as a heat-capacity standard. The samples, in the form of a flat disk, were loaded in a Pt crucible covered with a Pt lid. Pressing the samples in a disk ensured better compaction of the samples and therefore better thermal conductivity, better reproducibility of the sample shape, better contact with the bottom of the Pt crucible, and overall improved reproducibility of the heat-capacity data. The scans were performed in an atmosphere of flowing He (40 mL/min, low-temperature DSC) or Ar (50 mL/min, high-temperature DSC). Heat capacity was calculated by the software package supplied by the manufacturer.

Thermogravimetric analysis was performed with a Netzsch 449 TGA/DTA apparatus. The sample was continuously heated from room temperature up to 1000 K at a rate of 10 K/min in a stream of argon (50 mL/min). The proper operation of the instrument was checked by repeated measurement of weight loss of $CaC_2O_4 \cdot H_2O$.

2.7. Ion Chromatography

Approximately 5 mg of K_2SO_4 was dissolved in ~5 g of $3Na_2O \cdot 4MoO_3$ held at 975 K in a muffle furnace. The sample was quenched and dissolved in 50 mL of deionized water. The solutions were analyzed by ion chromatography by a procedure optimized for measurement of 0 to 300 ppm of sulfate in solution.

3. RESULTS

3.1. Characterization of Solid Samples

All samples used in this study produced sharp XRD patterns. Only the diffraction peaks of the major phase were discernible in each case. The lattice parameters of the sulfates, as determined by Rietveld refinement of the XRD patterns, are listed in Table 2. The starting crystal structure model for the refinement of anglesite, barite, and celestine was taken from Jacobsen et al. (1998). The starting model for anhydrite was taken from Hawthorne and Ferguson (1975), and the model for arcanite was taken from McGinnety (1972). The chemical composition of the two natural barite samples is listed in Table 3. Upon heating, the synthetic barite sample lost 2.46 wt%.

3.2. Investigation of the Final State of the Solvent

In high-temperature oxide melt calorimetry, a suitable final state of the solvent is a state with chemical species either completely expelled from the solvent (e.g., H_2O, CO_2;

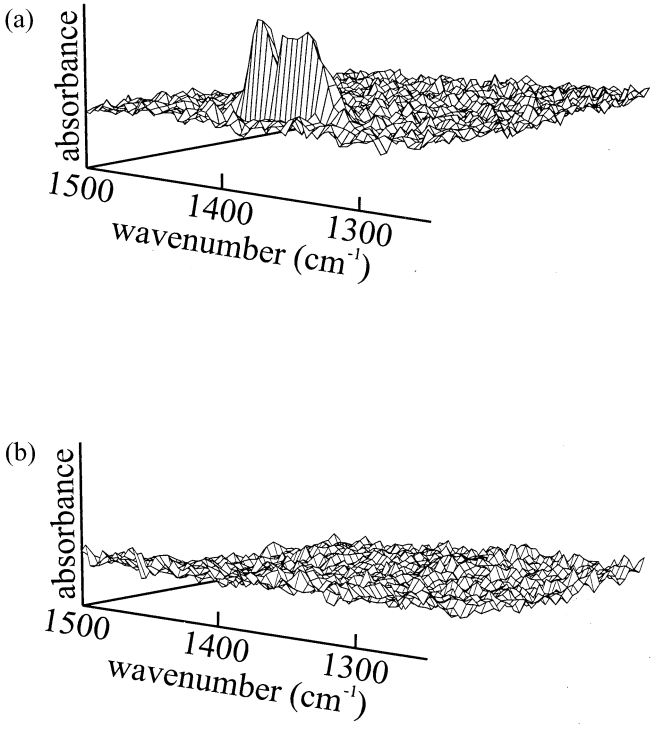

Fig. 3. FTIR spectra collected during evolution of 15 μg of SO_2 from decomposition of pyrite (a) and during dissolution of 32.06 mg of K_2SO_4 in molten $3Na_2O \cdot 4MoO_3$ calorimetric solvent (b). Both figures are drawn on the same scale.

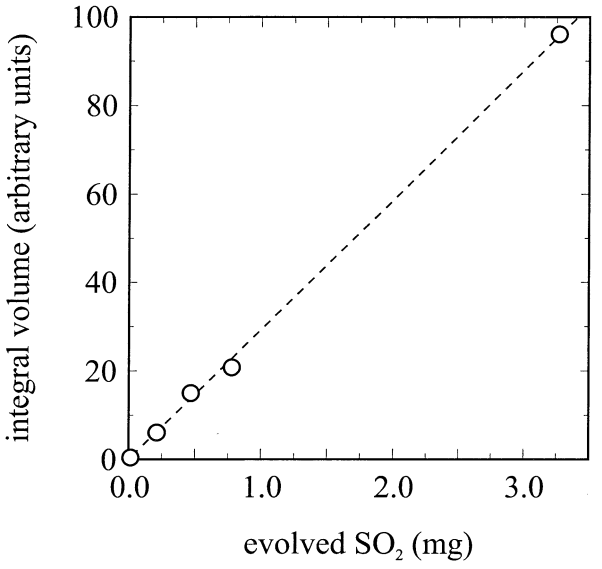

Fig. 4. Integral volume of the spectral region 1280 to 1420 cm^{-1} in the FTIR spectra as a function of amount of SO_2 that passed through the gas cell of the FTIR spectrometer.

Table 4. Enthalpies of drop solution (ΔH_{dsol}) of calorimetric samples.

Sample	ΔH_{dsol} (kJ/mol)
Anglesite	76.72[a] ± 1.11[b](17)[c]
Anhydrite	108.44 ± 0.66(13)
Arcanite	158.43 ± 1.06(20)
Barite (Colorado)	132.31 ± 1.19(8)
	132.69 ± 1.19[d]
Barite (South Calolina)	133.06 ± 0.98(9)
	133.43 ± 0.98[d]
Barite (synthetic)	150.75 ± 1.11(15)
	128.18 ± 1.11[e]
Celestine	124.82 ± 0.82(14)
Cerussite	100.24 ± 1.34(11)
Hematite	95.63 ± 0.50(27)
K_2CO_3	108.87 ± 1.02(10)
Lime	−91.50 ± 0.85(14)
Litharge	−15.39 ± 1.14(7)
Strontianite	128.72 ± 0.97(16)
Witherite	116.74 ± 1.28(18)

[a] Average.
[b] Two standard deviations of the mean.
[c] Number of experiments.
[d] Corrected for strontium impurity.
[e] Corrected for water impurity.

Navrotsky et al., 1994) or entirely retained in the solvent (most metal oxides). Corrections for partially dissolved species are unreliable. Moreover, the final speciation must be independent of the composition of the solid samples—for example, the sulfur species must be identical irrespective of which sulfate is used in the experiment. Preliminary analyses of the solvent with dissolved sulfates have shown that most sulfur remains in the solvent. Therefore, we concentrated on proving that all sulfur is retained by the solvent.

Chemical analyses of the solvent with dissolved sulfates showed that 99.7 ± 5.1 wt% (2σ) (six experiments) of sulfur is retained by the solvent. The large uncertainty on the determined value is due to the low concentration of sulfur in the analyzed solution (~60 ppm) and large concentration of the interfering molybdate ion.

FTIR spectrometry of the gas from the headspace above the solvent complemented the chemical analyses of the solvent. If all sulfur remains in the solvent, then no sulfur-bearing gases should be detected during the dissolution of sulfates. In each FTIR experiment, 70 spectra were collected during approximately 30 min (Fig. 3). The volume enclosed by the successive spectra in the range of 1280 to 1420 cm^{-1} (the stretching bands of SO_2) was integrated for each experiment and is reported (Fig. 4) in arbitrary units (a.u.). The integral volume varied by ± 0.9 a.u. during blank experiments when no sample was introduced in the assembly. The spectrometer response to variable amount of SO_2 passing through the gas cell was explored in experiments with pyrite decomposition (Fig. 3). The amount of SO_2 generated was calculated from the known weight of the sample assuming pyrite stoichiometry FeS_2 and complete conversion of sulfur in pyrite to SO_2. A linear fit ($r^2 = 0.999$) (Fig. 4) relates the integral volume of the spectra to the calculated amount of SO_2. A series of featureless spectra was observed during the dissolution of 32.06 mg of K_2SO_4 in the sodium molybdate solvent (Fig. 3). The integral volume (0.085 a.u.) corresponds to the evolution of 2.9 μg of SO_2, or 0.025 wt% of

Table 5. Thermochemical cycle for calculating the enthalpies of drop solution of SO_3 (Me = Ba, Ca, K_2, Pb, Sr).

	Reaction number and reaction	Enthalpy change
	sulfate-carbonate pairs	
1	SO_3 (g,298) = SO_3 (sol,975)	$\Delta H_1 = \Delta H_{dsol}(SO_3) = -\Delta H_2 - \Delta H_3 + \Delta H_4 + \Delta H_5 + \Delta H_6$
2	$MeCO_3$ (s,298) = MeO (sol,975) + CO_2 (g,975)	$\Delta H_2 = \Delta H_{dsol}(MeCO_3)$[a]
3	MeO (s,298) + CO_2 (g,298) = $MeCO_3$ (s,298)	$\Delta H_3 = \Delta H^o_{f,oxides}(MeCO_3)$[b]
4	CO_2 (g,298) = CO_2 (g,975)	$\Delta H_4 = H_{975} - H_{298}$ (CO_2)[b]
5	$MeSO_4$ (s,298) = MeO (sol,975) + SO_3 (sol,975)	$\Delta H_5 = \Delta H_{dsol}(MeSO_4)$[a]
6	MeO (s,298) + SO_3 (g,298) = $MeSO_4$ (s,298)	$\Delta H_6 = \Delta H^o_{f,oxides}(MeSO_4)$[b]
	sulfate-oxide pairs	
1	SO_3 (g,298) = SO_3 (sol,975)	$\Delta H_1 = \Delta H_{dsol}(SO_3) = -\Delta H_2 + \Delta H_5 + \Delta H_6$
2	MeO (s,298) = MeO (sol,298)	$\Delta H_2 = \Delta H_{dsol}(MeO)$[a]
5	$MeSO_4$(s,298) = MeO (sol,975) + SO_3 (sol,975)	$\Delta H_5 = \Delta H_{dsol}(MeSO_4)$[a]
6	MeO (s,298) + SO_3 (g,298) = $MeSO_4$ (s,298)	$\Delta H_6 = \Delta H^o_{f,oxides}(MeSO_4)$[b]

[a] Experimental data in Table 4.
[b] Calculated from Robie and Hemingway (1995).

Table 6. Enthalpy of drop solution of SO_3 ($\Delta H_{dsol}(SO_3)$) (kJ/mol) for individual sulfate-carbonate and sulfate-oxide pairs.

Sulfate-carbonate or sulfate-oxide	$\Delta H_{dsol}(SO_3)$
Anglesite-litharge	−213.2 ± 2.4
Anhydrite-lime	−203.7 ± 4.5
Arcanite-K_2CO_3	−203.7 ± 4.0
Barite-witherite (barite, Colorado)	−211.8 ± 4.1
Barite-witherite (barite, South Carolina)	−212.1 ± 4.1
Barite-witherite (synthetic barite)	−217.0 ± 4.1
Celestine-strontianite	−204.1 ± 4.9

the theoretical SO_2 content of 32.06 mg of K_2SO_4. Within the fluctuations of the blank runs, the amount of evolved SO_2 is zero.

The calculation of enthalpy of drop solution of SO_3 ($\Delta H_{dsol}(SO_3)$) tests the assumption of uniform speciation of sulfur in the solvent. Given (a) the presence of sulfur as $SO_4^{=}$ in the sulfates, (b) complete retention of sulfur in the solvent, and (c) constant temperature of the calorimeter, then the sulfur speciation in the solvent is the sole parameter affecting the value of $\Delta H_{dsol}(SO_3)$. $\Delta H_{dsol}(SO_3)$ cannot be determined directly experimentally but can be calculated by use of our experimental data (Table 4). The thermochemical cycle used for calculation of $\Delta H_{dsol}(SO_3)$ is given in Table 5. The agreement among the $\Delta H_{dsol}(SO_3)$ values for the individual sulfates (Table 6) is good and the sources of variation in the calculated data are discussed below. The enthalpy of drop solution and the enthalpy of solution of SO_3 is strongly exothermic, as expected, because the SO_3 molecule is acidic and unstable in the gas phase; its transformation to an SO_4^{2-} anion and solvation should be energetically favorable, as shown by our data. The large exothermic $\Delta H_{dsol}(SO_3)$ provides another qualitative argument supporting our conclusion that sulfate is retained by the solvent.

3.3. Enthalpy of Formation

The measured ΔH_{dsol} values (Table 4) displayed the normally encountered scatter around a mean value, with no signs of solvent saturation or departure from the Henrian behavior of the solute. The enthalpies of formation of the sulfates were calculated from the ΔH_{dsol} via a thermochemical cycle (Table 7). Arcanite (K_2SO_4) was chosen as the reference sulfate in the thermochemical cycle because its ΔH_f^o has been determined reliably from solution calorimetric experiments (Chase, 1998). The precision of high-temperature calorimetry is 0.6 to 1.4% (2σ) of the measured heat effect—that is, <1.5 kJ/mol (Table 4). The accuracy was tested by frequent measurement of ΔH_{dsol} of hematite. The sum of enthalpy changes for reactions listed in Table 8 must be equal to zero because enthalpy is a state function; the sum is −0.8 ± 0.7 kJ/mol. The magnitude of inaccuracy of the ΔH_{dsol} data is therefore approximately equal to the magnitude of imprecision of the data. The principal source of errors on ΔH_f^o (Table 9) are the errors on ΔH_f^o for carbonates or oxides (Robie and Hemingway, 1995) that are necessary for completion of the thermochemical cycle (Table 7).

Three reference lead-containing compounds, litharge (tetragonal PbO), massicot (orthorhombic PbO), and cerussite ($PbCO_3$), were measured. The ΔH_{dsol}(PbO,Q) (Q = tetragonal) measured on litharge is −15.39 ± 1.14 kJ/mol as compared with the ΔH_{dsol}(PbO,Q) of −18.52 ± 1.97 kJ/mol calculated from $\Delta H_{dsol}(PbCO_3)$ by using additional data (H_{975}-$H_{298}(CO_2)$, $\Delta H_f^o(PbCO_3)$) (Robie and Hemingway, 1995). Rane and Navrotsky (2001) measured $\Delta H_{dsol}(PbCO_3)$ and calculated the ΔH_{dsol}(PbO,Q) as −21.5 ± 1.5 kJ/mol. A massicot (orthorhombic PbO) sample gave ΔH_{dsol}(PbO,O) (O = orthorhombic) of −16.60 ± 0.91 kJ/mol. The sample is difficult to deal with because it partially transforms to tetragonal PbO upon

Table 7. Thermochemical cycle for calculation of enthalpy of formation of metal sulfate ($MeSO_4$, Me = Sr, Ba, Pb, Ca) from drop solution data.

Cycle	Reaction number and reaction	Enthalpy change
	K_2CO_3, K_2SO_4, $MeSO_4$, and metal carbonate ($MeCO_3$)	
1	Me (cr,298) + S (cr,298) + $2O_2$ (g,298) = $MeSO_4$ (cr,298)	$\Delta H_1 = \Delta H_f^o(MeSO_4) = -\Delta H_2 + \Delta H_3 + \Delta H_4 - \Delta H_5 + \Delta H_6 + \Delta H_7 - \Delta H_8$
2	K_2CO_3 (cr,298) = K_2O (sol,975) + CO_2 (g,975)	$\Delta H_2 = \Delta H_{dsol}(K_2CO_3)$[a]
3	K_2SO_4 (cr,298) = K_2O (sol,975) + SO_3 (sol,975)	$\Delta H_3 = \Delta H_{dsol}(K_2SO_4)$[a]
4	$MeCO_3$ (cr,298) = MeO (sol,975) + CO_2 (g,975)	$\Delta H_4 = \Delta H_{dsol}(MeCO_3)$[a]
5	$MeSO_4$ (cr,298) = MeO (sol,975) + SO_3 (sol,975)	$\Delta H_5 = \Delta H_{dsol}(MeSO_4)$[a]
6	Me (cr,298) + C (cr,298) + $3/2O_2$ (g,298) = $MeCO_3$ (cr,298)	$\Delta H_6 = \Delta H_f^o(MeCO_3)$[b]
7	2K (cr,298) + S (cr,298) + $2O_2$ (g,298) = K_2SO_4 (cr,298)	$\Delta H_7 = \Delta H_f^o(K_2SO_4)$[b]
8	2K (cr,298) + C (cr,298) + $3/2O_2$ (g,298) = K_2CO_3 (cr,298)	$\Delta H_8 = \Delta H_f^o(K_2CO_3)$[c]
	K_2CO_3, K_2SO_4, $MeSO_4$, and metal oxide (MeO)	
1	Me (cr,298) + S (cr,298) + $2O_2$ (g,298) = $MeSO_4$ (cr,298)	$\Delta H_1 = \Delta H_f^o(MeSO_4) = -\Delta H_2 + \Delta H_3 + \Delta H_4 - \Delta H_5 + \Delta H_6 + \Delta H_7 + \Delta H_8 + \Delta H_9$
2	K_2CO_3 (cr,298) = K_2O (sol,975) + CO_2 (g,975)	$\Delta H_2 = \Delta H_{dsol}(K_2CO_3)$[a]
3	K_2SO_4 (cr,298) = K_2O (sol,975) + SO_3 (sol,975)	$\Delta H_3 = \Delta H_{dsol}(K_2SO_4)$[a]
4	MeO (cr,298) = MeO (sol,975)	$\Delta H_4 = \Delta H_{dsol}(MeO)$[a]
5	$MeSO_4$ (cr,298) = MeO (sol,975) + SO_3 (sol,975)	$\Delta H_5 = \Delta H_{dsol}(MeSO_4)$[a]
6	CO_2 (g,298) = CO_2 (g,975)	$\Delta H_6 = \Delta H_{975} - H_{298}(CO_2)$[b]
7	K_2CO_3 (cr,298) + SO_3 (g,298) = K_2SO_4 (cr,298) + CO_2 (g,298)	$\Delta H_7 = \Delta H_{rxn}$[b]
8	Me (cr,298) + $1/2O_2$ (g,298) = MeO (cr,298)	$\Delta H_8 = \Delta H_f^o(MeO)$[b]
9	S (cr,298) + $3/2O_2$ (g,298) = SO_3 (g,298)	$\Delta H_9 = \Delta H_f^o(SO_3)$[b]

[a] Experimental data in Table 4.
[b] Taken or calculated from Robie and Hemingway (1995).
[c] Chase (1998).

Table 8. Thermochemical cycle for assessing the accuracy of high-temperature calorimetry.

Reaction	Enthalpy	Reference
Fe_2O_3 (cr,298) = Fe_2O_3 (cr,975)	$H_{975}-H_{298}$ = 96.86 ± 0.45	Majzlan (unpublished data)
Fe_2O_3 (cr,975) = Fe_2O_3 (sol,975)	ΔH_{sol} = −2.05 ± 0.21	Navrotsky and Kleppa (1968)
Fe_2O_3 (sol,975) = Fe_2O_3 (cr,298)	$-\Delta H_{dsol}$ = −95.63 ± 0.50	This study (Table 4)

pressing into a pellet. An XRD analysis showed that this sample is still predominantly orthorhombic PbO. Combining the ΔH_{dsol} (PbO,O) with enthalpy of PbO(Q) = PbO(O) transformation at 298.15 K (−1.7 ± 0.9 kJ/mol; Robie and Hemingway, 1995), we arrive at ΔH_{dsol}(PbO,Q) of −14.9 ± 1.3 kJ/mol, in excellent agreement with the measured ΔH_{dsol}(PbO,Q) value. In this study, we use the ΔH_{dsol}(PbO,Q) measured on the tetragonal PbO (litharge) although this value yields the poorest agreement of our $\Delta H_f^o(PbSO_4)$ with the tabulated data (Robie and Hemingway, 1995). The ΔH_{dsol}(PbO,Q) value was chosen because no additional thermodynamic data are required to constrain it. The data scatter led us to check the dissolution of the lead compounds in the calorimetric solvent, in particular whether a $PbMoO_4$ precipitate might form and cause an irreproducible final state. However, synthetic $PbMoO_4$ dissolved in the solvent both rapidly and in quantities exceeding the lead concentration encountered in our calorimetric experiments. There is no evidence for precipitation or other problems in calorimetry of lead compounds.

The ΔH_{dsol}(barite) values must be corrected for the strontium and water impurity for the natural and synthetic barite, respectively. The correction for strontium (0.3% correction) was done assuming ideal solid solution between barite and celestine. Although disagreement exists about ideal (Brower and Renault, 1977) vs. non-ideal behavior of this solid solution (Becker et al., 2000; Kotel'nikov et al., 2000), the persistence of a continuous solid solution at ambient temperature suggest that the deviation from ideality, if any, is small. The small concentration of the $SrSO_4$ end member in the natural end-member should therefore result in a negligible error arising from the assumption of ideality. The correction for the water impurity (15% correction) in the synthetic barite sample is substantial (cf. Table 4). The correction was made with an assumption that the impurity is a) pure water, and b) present in microscopic fluid inclusions. Both assumptions are likely incorrect. If inclusions were trapped, they would contain the mother solution rich in Na^+ and NO_3^-. The significant difference between the lattice parameters of the natural and synthetic barite (Table 2) suggests that the water (as H_2O or OH^-) is present in the structure of the sample. Because the actual composition and position of the impurity in the structure is unknown, we consider all data derived for the synthetic barite unreliable.

Table 9. Enthalpies of formation of sulfates (ΔH_f^o) from the elements.

Sample	ΔH_f^o(kJ/mol)
Anglesite	−909.9 ± 3.4
Anhydrite	−1433.8 ± 3.2
Barite (Colorado)	−1464.2 ± 3.7
Barite (South Carolina)	−1464.9 ± 3.7
Barite (synthetic)	−1459.7 ± 3.7
Celestine	−1452.1 ± 3.3

3.4. Heat Capacity and Heat Content

The results of heat-capacity (C_p) measurements (Figs. 5a–c) were averaged and fitted to a Haas-Fisher polynomial $C_p(T) = a + bT + cT^{-2} + dT^{-0.5} + eT^2$ (Table 10). The same table indicates the 95% confidence interval (two standard deviations of the mean) for all C_p curves. For the measurement of C_p(barite), only the natural sample (South Carolina) was used. The C_p(barite) was not corrected for the strontium content of the natural barite because the individual runs on C_p(barite) and C_p(celestine) overlap and the correction for the small Sr content is insignificant. Heat content (H_{975}-H_{298}, H_{1075}-H_{298}) was measured for the same sulfate samples (Table 11) for which C_p data are reported. The accuracy of the heat content measurement was tested by measuring heat content of quartz (Table 11). The measured heat content is also compared with the $\int_{298}^{975} C_p dT$ and $\int_{298}^{1075} C_p dT$ values calculated from C_p data derived in this study and the C_p equations of Robie and Hemingway (1995), showing good mutual agreement of the heat content and integrated C_p measured in this study.

4. DISCUSSION

To establish high-temperature oxide melt calorimetry as a technique suitable for studying the energetics of sulfates, complete retention of sulfur in the solvent has to be documented. The evidence of full retention is provided by chemical analyses of the solvent and the FTIR analysis of the gases above the solvent. Possible inconsistencies and sources of error in the tabulated and presented thermodynamic data that contribute to the scatter in the $\Delta H_{dsol}(SO_3)$ values (Table 6) are discussed below.

The tabulated ΔH_f^o of barite vary between −1473.6 and −1457.4 kJ/mol. Robie and Hemingway (1995) (−1473.6 ± 1.0 kJ/mol) refer to DeKock (1986) (−1473.6) who adopted the value given by Parker et al. (1971) (−1473.2) with a small correction. Parker et al. (1971) did not specify the original reference. The thermodynamic compilation of Helgeson et al. (1978) and Robie et al. (1978) also refer to Parker et al. (1971). Nordstrom and Munoz (1994) calculated ΔH_f^o of barite (−1468.3 ± 2.5) from selected ΔH_f^o values of Ba^{2+}, $SO_4^=$, and enthalpy of dissolution of barite. The tables of Naumov et al. (1971) (−1457.4) refer to Kelley (1960), who gives only heat-capacity data for barite. A number of references to ΔH_f^o, with no specification as to which ones were used and in what way, can be found in the tabulations of Rossini et al. (1952) (−1465.2) and Glushko (1979) (−1458.9 ± 2.2). Only the ΔH_f^o value of Nordstrom and Munoz (1994) can be traced to its original sources. We were unable to find an original paper that

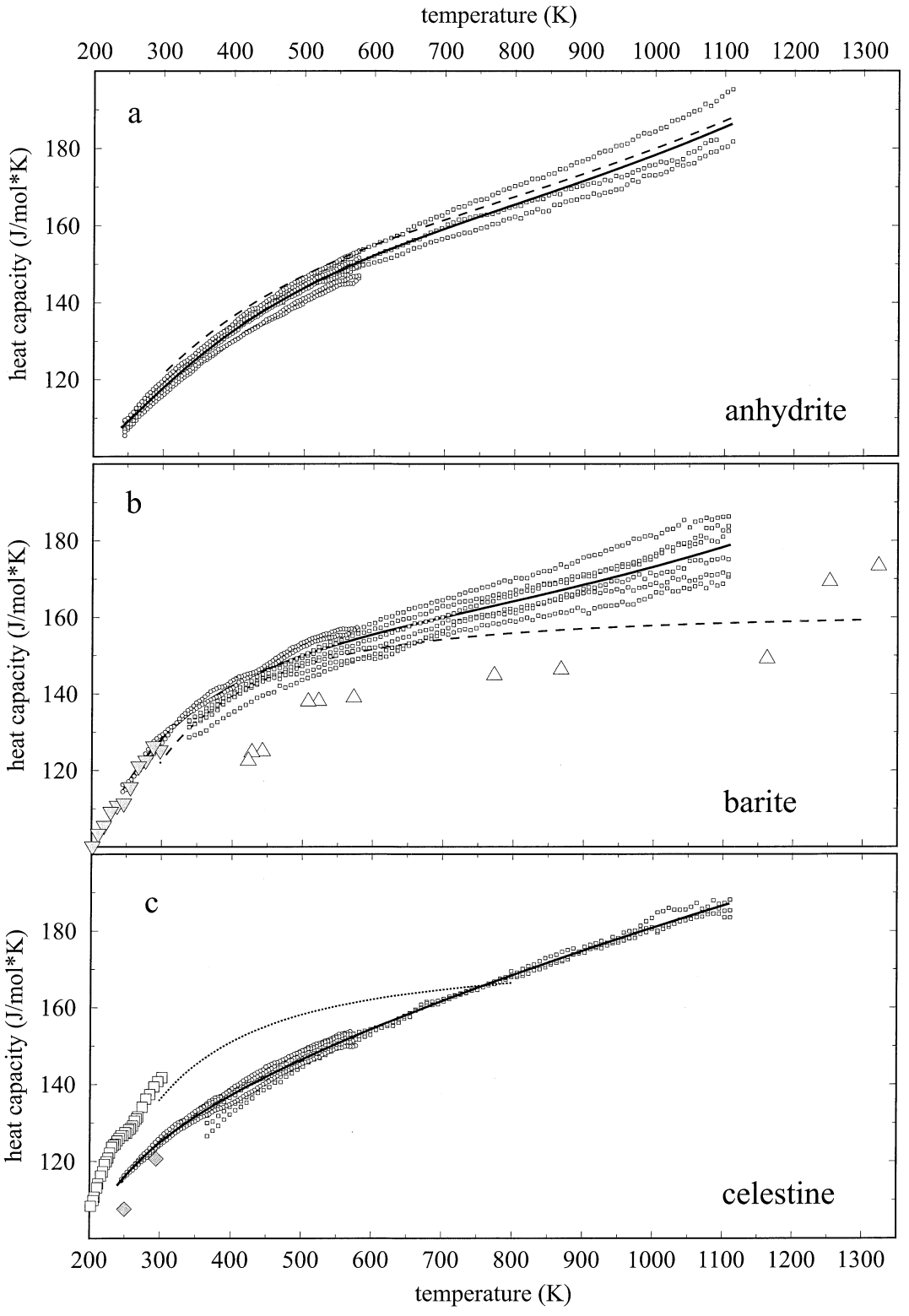

Fig. 5. Heat-capacity data for (a) anhydrite, (b) barite, and (c) celestine. All figures have the same horizontal scale. The DSC data (small symbols) (this work) are fitted to a Haas-Fisher polynomial (thick solid line). The C_p polynomial from Robie and Hemingway (1995) (dashed line) and Kotel'nikov et al. (2000) (dotted line) are shown for comparison. Large symbols: open squares = Gurevich et al. (1997); gray diamonds = Sakamoto (1954); open triangles = Lashchenko (1910); gray inverted triangles = Latimer et al. (1933).

Table 10. Coefficients of the Haas-Fisher heat capacity polynomial $C_p(T) = a + bT + cT^2 + dT^{-0.5} + eT^2$ for the sulfate samples (valid between 245 and 1100 K). The last column shows the relative uncertainty (two standard deviations of the mean) of the measured C_p value at the low temperature and high temperature end, respectively.

Sample	a	b × 10^1	c × 10^{-6}	d × 10^{-3}	e × 10^5	2σ
Anhydrite	409.7	−1.764	2.672	−5.130	8.460	1%, 5%
Barite[a]	230.5	−0.7395	−1.170	−1.587	4.784	2%, 4%
Celestine	82.1	0.8831	−1.213	0.1890	−1.449	1%, 2%

[a] Barite from South Carolina.

gives enthalpy of formation of barite. On the other hand, there is a wealth of reported dissolution enthalpies of barite from dissolution/precipitation experiments (Table 12). These values show much smaller scatter (5.8 kJ/mol) than ΔH_f^o (barite) (16.2 kJ/mol). By use of the ΔH_f^o for Ba^{2+} (−532.5 ± 2.5 kJ/mol) and $SO_4^{=}$(−909.3 ± 0.4) (Cox et al., 1989), and the $\Delta H_{dissolution}$ in Table 12 (excluding the value of Paige et al., 1998, which lies almost 4σ away from the mean), the computed ΔH_f^o (barite) range is −1468.4 ± 2.5 to −1462.6 ± 2.5 kJ/mol. The ΔH_f^o determined in this study (for the natural barite samples) and the value estimated by Nordstrom and Munoz (1994) are, in our opinion, a better estimate ΔH_f^o value than the ΔH_f^o of Robie and Hemingway (1995).

The preparation procedure of barite samples can significantly influence the measured thermodynamic properties (Blount, 1977; Paige et al., 1998). Only a few studies summarized in Table 12 paid special attention to characterization of their barite sample. Fine-grained barite particles readily precipitate during mixing of barium nitrate or chloride solution with a solution of soluble sulfate or sulfuric acid. In this study, fine-grained $BaSO_4$ precipitates were avoided because they are difficult to characterize and cannot be guaranteed to be pure without significant analytical effort. Despite the fact that the barite synthesized in this study appears to be phase pure according to the XRD pattern, the ΔH_f^o of synthetic barite significantly deviates from ΔH_f^o of the natural barite (Table 9). Although the crystals of synthetic gypsum (Fig. 1a), celestine (Fig. 1b), and anglesite (Fig. 1c) are euhedral, the synthetic crystals of barite (Fig. 1d) are dendritic, suggesting rapid crystallization and trapping of inclusions of solution or other impurities. Hence, fine-grained precipitates of sparingly soluble sulfates are inadequate as samples for thermodynamic investigations.

Anhydrite served as a reference sample during the heat-capacity measurements (Fig. 5a) because its heat capacity was measured relatively recently by Robie et al. (1989) and found to be in good agreement with experiments on the gypsum–anhydrite transition (Robie et al., 1989). The mean $C_p(CaSO_4)$ deviates from that of Robie et al. (1989) by almost 3.5% at the low temperature end, and falls smoothly to ~1% at the high temperature end. The accuracy of the low-temperature DSC data can be tested by calculating the equilibrium temperature of the gypsum–anhydrite transformation. By use of our DSC data, we arrive at a temperature of 314.1 K, essentially equal to the 314.7 ± 2.1 K of Robie et al. (1989). The agreement between measured heat content and integrated C_p data from this study (Table 11) suggests that the accuracy of our DSC data is satisfactory.

The heat capacity of barite measured in this study (Fig. 5b) joins smoothly the adiabatic calorimetry data of Latimer et al. (1933) but deviates significantly from the C_p polynomial of Robie and Hemingway (1995) at $T > 600$ K. The data of Lashchenko (1910), the only data set for C_p (barite) at $T > 300$ K, seem too scattered to constrain a C_p curve. Individual DSC runs on barite show larger scatter than the DSC runs on anhydrite and celestine, especially at high temperature. The standard entropy (S^o) is a function of low-temperature C_p and can be used to check the validity of different C_p curves. S^o (barite) was experimentally determined by Latimer et al. (1933) (131.8 J/mol/K) and calculated by Nordstrom and Munoz (1994) (128.6 J/mol/K). Assuming that the entropy change of the reaction (calcite + barite = witherite + anhydrite) is zero at near ambient temperature because reactants and products are crystalline solids, S^o (barite) = S^o (witherite) − S^o (calcite) + S^o (anhydrite). This calculation of S^o (barite) gives comparable values of 127.8 J/mol/K when the data in Robie and Hemingway (1995) are used, and 126.9 J/mol/K when the data from Nordstrom and Munoz (1994) are used.

Integrated C_p of celestine from this study compares well to the heat content measured directly by high-temperature calorimetry (Table 11), suggesting satisfactory accuracy of our DSC data. A comparison of our DSC data with the adiabatic calorimetry data of Gurevich et al. (1997) in the overlap range of 243 to 303 K (Fig. 5b) shows a systematic discrepancy of ~10%. The C_p(celestine) of Kotel'nikov et al. (2000) joins the adiabatic data of Gurevich et al. (1997). The heat capacity of celestine, calculated from vibrational density of states (Sakamoto, 1954) (Fig. 5b), is lower than our DSC data by ~3%. An analogous calculation from a simplified vibrational density of states of barite (Sakamoto, 1954) differs from the experimental C_p data (Latimer et al., 1933) by 0.7% on average. The tabulations of standard entropy of celestine vary from 117.0 ± 4.2 J/mol/K by Robie and Hemingway (1995), taken from Wagman et al. (1982) where no references are listed, 128.3 J/mol/K by Nordstrom and Munoz (1994), to 135.98 ± 0.25 J/mol/K by Gurevich et al. (1997). Assuming that the entropy change of the reaction (calcite + celestine = strontianite + anhydrite) is zero, we arrive at S^o (celestine) of 112.8 J/mol/K with the necessary data taken from Robie and Hemingway (1995), and 112.0 J/mol/K with data from Nordstrom and Munoz (1994). The range of standard entropies accounts for variation of 7 kJ/mol in ΔG_f^o at 298 K. A choice of the best value for $S^o(SrSO_4)$ would require revision of entropy data for $SrCO_3$, Sr^{2+}, or reversed equilibrium experiments at high temperature, both of these being beyond the scope of this paper.

A striking feature of the C_p(barite) (Robie and Hemingway, 1995) and C_p(celestine) (Kotel'nikov et al., 2000) curves (Fig. 5) is the apparent leveling-off at temperatures ~800 K. Vibra-

Table 11. Comparison of heat content measured by high-temperature calorimetry (H_T–H_{298}) with heat content calculated by integrating heat capacity polynomials ($\int^T C_p dT$) from this study or those of Robie and Hemingway (1995).

Phase/quantity	H_{975}–H_{298}, this study	$\int^{975} C_p dT$, this study	$\int^{975} C_p dT$, Robie and Hemingway (1995)
Anhydrite	90.40[a] ± 0.80[b] (11)[c]	89.70	91.54
Barite	87.62 ± 0.65 (10)[d]	91.48[e]	87.41
	87.55 ± 1.13 (8)[e]		
Celestine	88.92 ± 1.50 (9)	91.72	—
Quartz	42.30 ± 0.44 (10)	—	43.17
	H_{1075}–H_{298}, this study	$\int^{1075} C_p dT$, this study	$\int^{1075} C_p dT$, Robie and Hemingway (1995)
Anhydrite	104.75 ± 1.67 (9)	105.71	107.72

[a] Average.
[b] Two standard deviations of the mean.
[c] Number of measurements.
[d] Measured on barite from Colorado.
[e] Measured on barite from South Carolina.

tional contribution to the heat capacity of a crystalline solid (McQuarrie, 1976) can be calculated as

$$C_v = k \int [x^2 e^x/(e^x - 1)^2] g(\omega) d\omega$$

where $x = \hbar\omega/kT$, $g(\omega)$ is the vibrational density of states, ω is angular frequency, T is absolute temperature, and k and $\hbar$ are Boltzmann's constant and Planck's constant divided by 2π, respectively. This expression shows that the internal vibrational modes of the barite structure at 450 to 480, 600 to 650, 980 to 990, and 1050 to 1200 cm^{-1} (as reported by Dawson et al., 1977) will cause an increase in C_p beyond 1000 K. Therefore, leveling off of the C_p curve at 800 K is unlikely. A similar argument can be made for all sulfates isostructural with barite. Furthermore, the internal modes in the anhydrite structure appear at similar frequencies, and no leveling in C_p(anhydrite) was documented either in this study or by Robie et al. (1989). In short, the new data portray the heat capacity of barite and celestine more accurately than the previous data sets.

5. SUMMARY

Sulfur (introduced in the calorimeter in the form of sulfates) is fully retained by the calorimetric solvent ($3Na_2O \cdot 4MoO_3$) at 975 K. The full retention was confirmed by chemical analyses of the solvent and FTIR analyses of the gas above the solvent. The enthalpy of solution of SO_3 in the solvent is highly exothermic and independent of the crystalline sulfate phase used for the calorimetric experiments. Enthalpies of formation of several simple anhydrous sulfates determined in this study agreed well with the tabulated values (Nordstrom and Munoz, 1994; Robie and Hemingway, 1995). The observations above form the basis for the principal conclusion of this work that high-temperature oxide melt calorimetry is a technique suitable for studying the energetics of anhydrous sulfates. Our investigation will be extended to the solid solutions between Ba, Sr, and Pb sulfates. The feasibility of calorimetry on hydrous sulfates will be explored in further detail, especially with respect to possible interaction of water and sulfur during dissolution of the hydrous sulfates.

The enthalpy of formation of barite (natural samples) measured in this study is −1464.2 ± 3.7 and −1464.9 ± 3.7 kJ/mol. The values are in good agreement with a number of published $\Delta H_{dissolution}$ values, combined with ΔH_f^o of Ba^{2+} and $SO_4^{=}$ from Cox et al. (1989). The inconsistencies in the thermodynamic values derived for synthetic barite prepared from low-temperature aqueous solution imply that similar data should be used only with caution. The likely cause of problems when synthetic barite is used is the unavoidable trapping of the aqueous solution during the rapid crystal growth.

Table 12. Compilation of published enthalpies of dissolution of barite.

$\Delta H_{dissolution}$ (kJ/mol)	Reference	Measured quantity or method
23.01	Holleman (1893)	Conductance[a]
25.10	Melcher (1910)	Conductance[a]
22.82	Muller (1918)	Enthalpy of precipitation
24.29	Shibata and Terasaki (1936)	Enthalpy of precipitation
25.03	Singh (1954)	Solubility (no details given)[a]
23.05	Khodakovskiy et al. (1966)	Calculated from literature data
26.57	Blount (1977)	Solubility (XRF analyses of solutions)[a], and literature data
26.21	Raju and Atkinson (1988)	Calculated from literature data
26.5 ± 0.5	Nordstrom and Munoz (1994)	Calculated from literature data
17.6 ± 0.2	Paige et al. (1998)	^{133}Ba radio tracer, solubility[a]

[a] In these studies, enthalpy of dissolution was calculated from temperature dependence of barite solubility.

Acknowledgments—We thank S. Hollands for help in the initial stages of the project. We also thank Z. Munir for the permission to use and E. Carrillo-Heian (University of California–Davis) for assistance with the particle size distribution analyzer. We are grateful to B. McCleskey (USGS) for the analysis of sulfate in the sodium molybdate solvent. M. Dunlap (CHMS, University of California–Davis) took the scanning electron microscope photographs of the sulfate crystals. J. Bishop and an anonymous reviewer provided comments and suggestions that improved the quality of the manuscript. This study was supported by the U.S. Department of Energy (grant DE-FG0397SF 14749).

Associate editor: D. J. Wesolowski

REFERENCES

Baron D. and Palmer C. D. (1996) Solubility of jarosite at 4–35°C. *Geochim. Cosmochim. Acta* **60,** 185–195.

Becker U., Fernandez-Gonzalez A., Prieto M., Harrison R., and Putnis A. (2000) Direct calculation of the thermodynamic properties of the barite/celestite solid solution from molecular principles. *Phys. Chem. Miner.* **27,** 291–300.

Bennett N. L. (1986) The Stoneham barite locality, Colorado. *Mineral. Rec.* **17,** 255–258.

Blount C. W. (1977) Barite solubility and thermodynamic quantities up to 300°C and 1400 bars. *Am. Mineral.* **62,** 942–957.

Brobst D. A. (1983) Barium minerals. In *Industrial Minerals and Rocks* (ed. S. J. Lefond), 5th ed., Vol. 1, pp. 485–501. Society of Mining Engineers.

Brower E. and Renault J. (1977) Solubility and enthalpy of the barium–strontium sulfate solid solutions series. *New Mexico State Bur. Mines Mineral Res.* **116,** 1–21.

Chase M. W. Jr. (1998) *NIST-JANAF Thermochemical Tables*,4th ed. Monograph no. 9, part 1, p. 621; part 2, p. 1481. J. Phys. Chem. Ref. Data.

Cox J. D., Wagman D. D., and Medvedev V. A. (1989) *CODATA Key Values for Thermodynamics.* Hemisphere.

Dawson P., Hargreave M. M., and Wilkinson G. R. (1977) Polarized i.r. reflection, absorption and laser Raman studies on a single crystal of $BaSO_4$. *Spectrochim. Acta* **33A,** 83–93.

DeKock C. W. (1986) *Thermodynamic Properties of Selected Metal Sulfates and their Hydrates.*Circular 9081. U.S. Bureau of Mines Information.

Dutrizac J. E. and Jambor J. L. (2000) Jarosites and their application in hydrometallurgy. *Rev. Mineral. Geochem.* **40,** 405–452.

Fernelius W. C. and Detling K. D. (1934) Preparation of crystals of sparingly soluble salts. *J. Chem. Educ.* **11,** 176–178.

Glushko V. P. (ed.) (1979) *Termicheskie Konstanty Veshchestv,*Vol. 9. Akademia Nauk SSSR.

Gurevich V. M., Gavrichev K. S., Gorbunov V. E., Danilova T. V., and Khodakovkii I. L. (1997) Low-temperature heat capacity of celestine $SrSO_4$ (in Russian). *Geokhimiya* 305–311.

Härtig C., Brand P., and Bohmhammel K. (1984) Fe-Al Isomorphie und Strukturwasser in Kristallen von Jarosit-Alunit-Typ. *Z. Anorg. Allg. Chem.* **508,** 159–164.

Hawthorne F. C. and Ferguson R. B. (1975) Anhydrous sulphates. II. Refinement of the crystal structure of anhydrite. *Can. Mineral.* **13,** 289–292.

Hawthorne F. C., Krivovichev S. V., and Burns P. C. (2000) The crystal chemistry of sulfate minerals. *Rev. Mineral. Geoch.* **40**, 1–112.

Helgeson H. C., Delany J. M., Nesbitt H. W., and Bird D. K. (1978) Summary and critique of the thermodynamic properties of rock-forming minerals. *Am. J. Sci.* **278A**, 229 pp.

Holleman A. F. (1893) Bestimmungen der Löslichkeit sogenannter unlöslicher Salze. *Z. Phys. Chem.* **12,** 125–139.

Horton J. W. Jr. (1989) Barite in quartz–sericite schist and schistose pyroclastic rock of the Battleground formation, Kings Mountain Belt. In *Mineral Resources of the Charlotte 1° × 2° Quadrangle, North Carolina and South Carolina* (ed. J. E. Gair), pp. 115–118. Professional Paper 1462. U.S. Geological Survey.

Jacobsen S. D., Smyth J. R., Swope R. J., and Downs R. J. (1998) Rigid-body character of the SO_4 groups in celestine, anglesite, and barite. *Can. Mineral.* **36,** 1053–1060.

Kelley K. K. (1960) Contributions to the data on theoretical metallurgy XIII: High-temperature heat-content, heat-capacity, and entropy data for the elements and inorganic compounds. *Bureau Mines Bull.* **584**, 232 pp.

Khodakovskiy I. L., Mishin I. V., and Zhogina V. V. (1966) About temperature dependence of solubility constants and some limits on the chemical composition of hydrothermal solutions (in Russian). *Geokhimiya* 861–866.

Kotel'nikov A. R., Kabalov Yu. K., Zezulya T. N., Mel'chakova L. V., and Ogorodova L. P. (2000) Experimental study of a celestite–barite solid solution. *Geokhimiya* **12,** 1286–1293.

Larson A. C. and von Dreele R. B. (1994) *GSAS: General Structure Analysis System*. LANSCE, MS-H805.

Lashchenko P. N. (1910) About the high-temperature heat capacities of barite, witherite, fused lime, quartz, and chalcedony (in Russian). *J. Russ. Phys. Chem. Soc.* **42,** 1604–1614.

Latimer W. M., Hicks J. F. G., and Schutz P. W. (1933) The heat capacities and entropies of calcium and barium sulfates from 15 to 300°K. The entropy and free energy of sulfate ion. *J. Chem. Phys.* **1,** 620–624.

McGinnety J. A. (1972) Redetermination of the structures of potassium sulphate and potassium chromate: The effect of electrostatic crystal forces upon observed bond lengths. *Acta Cryst.* **B28,** 2845–2852.

McQuarrie D. A. (1976) *Statistical Mechanics*. HarperCollins.

Melcher A. C. (1910) The solubility of silver chloride, barium sulphate, and calcium sulphate at high temperatures. *J. Am. Chem. Soc.* **32,** 50–66.

Muller J.-A. (1918) Sur la chaleur d'ionisation, en solution aqueuse, du sulfate de baryum cristallise et sur la solubilite de ce sel dans l'eau. *Bull. Soc. Chim. Fr. Ser. 4* **23,** 13–16.

Myneni S. C. B. (2000) X-ray and vibrational spectroscopy of sulfate in earth materials. *Rev. Mineral. Geochem.* **40,** 113–172.

Naumov G. B., Ryzhenko B. N., and Khodakovsky I. L. (1971) *Handbook of Thermodynamic Data*. Atomizdat.

Navrotsky A. (1997) Progress and new directions in high temperature calorimetry revisited. *Phys. Chem. Mineral.* **24,** 222–241.

Navrotsky A. and Kleppa O. J. (1968) Thermodynamics of formation of simple spinels. *J. Inorg. Nucl. Chem.* **30,** 479–498.

Navrotsky A., Rapp R. P., Smelik E., Burnley P., Circone S., Liang C., and Kunal B. (1994) The behavior of H_2O and CO_2 in high-temperature lead borate solution calorimetry of volatile-bearing phases. *Am. Mineral.* **79,** 1099–1109.

Nordstrom D. K. and Munoz J. L. (1994) *Geochemical Thermodynamics.* Blackwell Scientific.

Paige C. R., Kornicker W. A., Hileman O. E. Jr., and Snodgrass W. J. (1998) Solution equilibria for uranium ore processing: The $BaSO_4$-H_2SO_4-H_2O system and the $RaSO_4$-H_2SO_4-H_2O system. *Geochim. Cosmochim. Acta* **62,** 15–23.

Parker V. B., Wagman D. D., and Evans W. H. (1971) Selected values of chemical thermodynamic properties. Tables for the alkaline earth elements (elements 92 through 96 in the standard order of arrangement). *NBS Tech. Note* **270,** 6.

Raju K. and Atkinson G. (1988) Thermodynamics of "scale" mineral solubilities. I. $BaSO_4$(s) in H_2O and aqueous NaCl. *J. Chem. Eng. Data.* **33,** 490–495.

Rane M. V. and Navrotsky A. (in press) Enthalpies of formation of lead zirconate titanate (PZT) solid solutions. *J. Solid State Chem.*

Rimstidt J. D. (1997) Gangue mineral transport and deposition. In *Geochemistry of Hydrothermal Ore Deposits* (ed. H. L. Barnes), pp. 487–515. 3rd ed. Wiley.

Robie R. A., Hemingway B. S., and Fisher J. R. (1978) *Thermodynamic Properties of Minerals and Related Substances at 298.15 K and 1 bar (10^5 pascals) and at Higher Temperatures.* Bulletin 1452. U.S. Geological Survey.

Robie R. A., Russell-Robinson S., and Hemingway B. S. (1989) Heat capacities and entropies from 8 to 1000 K of langbeinite ($K_2Mg_2(SO_4)_3$), anhydrite ($CaSO_4$) and of gypsum ($CaSO_4 \cdot 2H_2O$) to 325 K. *Thermochim. Acta* **139,** 67–81.

Robie R. A. and Hemingway B. S. (1995) *Thermodynamic Properties of Minerals and Related Substances at 298.15 K and 1 bar (10^5 pascals) and at Higher Temperatures.* Bulletin 2131. U.S. Geological Survey.

Rossini F. D., Wagman D. D., Evans W. H., Levine S., and Jaffe I.

(1952) *Selected Values of Chemical Thermodynamic Properties.* NBS Circ. 500. U.S. Department of Commerce.

Sakamoto Y. (1954) Analytic treatment of the C_p-T relation for the crystal of $BaSO_4$, $CaSO_4$, $PbSO_4$, and $SrSO_4$. *J. Sci. Hiroshima Univ. Ser. A* **17,** 397–405.

Shibata Z. and Terasaki Y. (1936) Thermochemical study of inorganic compounds by using non-constant temperature adiabatic calorimeter: Measurements of hydration enthalpy for barium chloride and the first solution enthalpy for barium sulfate (in Japanese). *Bull. Chem. Soc. Jpn.* **57,** 1212–1216.

Singh D. (1954) Standard entropy of the sulphate ion from solubilities of its sparingly soluble salts. *J. Sci. Res. Banaras Hindu Univ.* **6,** 131–132.

Stoffregen R. E. (1993) Stability relations of jarosite and natrojarosite. *Geochim. Cosmochim. Acta* **57,** 2417–2419.

Wagman D. D., Evans W. H., Parker V. B., Schumm R. H., Halow I., Bailey S. M., Churney K. L., and Nuttal R. L. (1982) The NBS tables of chemical thermodynamic properties. Selected values for inorganic and C_1 and C_2 organic substances in SI units. *J. Phys. Chem. Ref. Data* **11(Suppl. 2),** 1–392.